Abdominal Imaging

Published online: 18 December 2011

Abdom Imaging (2012) 37:767–774
DOI: 10.1007/s00261-011-9833-7

Malignant versus benign hepatic masses in patients with recurrent pyogenic cholangitis: MR differential diagnosis

Hyo Won Eun,[1] Jung Hoon Kim,[2] Seong Sook Hong,[3] Young Jae Kim[3]

[1]Health Promotion Center, Asan Medical Center, University of Ulsan, 388-1 Poongnap-dong, Songpa-gu, Seoul 138-736, Korea
[2]Department of Radiology and Institute of Radiation Medicine, Seoul National University College of Medicine, 101 Daehang-no, Chongno-gu, Seoul 110-744, Korea
[3]Department of Radiology, Soonchunhyang University Hospital, 657 Hannam-Dong, Youngsan-Ku, Seoul 140-743, Korea

Abstract

Purpose: To assess MR findings and diagnostic performance for differentiating malignant from benign hepatic masses in recurrent pyogenic cholangitis (RPC).
Materials and methods: During a recent 6-year period, we performed MRI in 352 patients with RPC. Among them, 58 had confirmed hepatic masses; cholangiocarcinoma ($n = 15$), abscess ($n = 37$), inflammatory pseudotumor ($n = 3$), biloma ($n = 3$). Two radiologists assessed MR findings including enhancement patterns, intratumoral appearance, peritumoral changes, mass location, and multiplicity. They also graded the malignancy using common MR findings. The receiver operating characteristic analysis and Chi-square test were used. The κ statistics was used to determine interobserver agreement.
Results: The common findings for cholangiocarcinoma were thin and lobulated enhancement at the periphery ($n = 8$, 53%, $P < 0.05$); ill-defined enhancement ($n = 7$, 47%, $P < 0.05$); slightly high signal on T2 ($n = 13$, 87%, $P < 0.05$); mass located in the same lobe of atrophy ($n = 11$, 73%, $P < 0.05$) and portal vein thrombosis ($n = 15$, 100%, $P < 0.05$). The common findings for benign mass were target-like enhancement ($n = 36$, 84%, $P < 0.05$); cluster appearance ($n = 15$, 35%, $P < 0.05$); central, fluid-like space ($n = 29$, 67%, $P < 0.05$); peritumoral regional high signal on T2 ($n = 32$, 74%, $P < 0.05$); multiplicity($n = 21$, 49%, $P < 0.05$). Interobserver agreement was excellent ($\kappa = 0.81$–1.000). Area under the curve (Az) for differentiating malignant masses was 0.989, sensitivity was 95.3%, and specificity was 95.3%. There was good interobserver agreement ($\kappa = 0.74$).
Conclusion: MR imaging is very useful for differential diagnosis of malignant vs. benign hepatic masses in patients with RPC.

Key words: Biliary system—Pyogenic cholangitis—Cancer—Cholangiocarcinoma—Abscess—MRI

Correspondence to: Jung Hoon Kim; *email:* Jhkim2008@gmail.com

Recurrent pyogenic cholangitis (RPC) is a complex biliary tract disease characterized by intrahepatic pigment stones. RPC is characterized clinically by recurrent attacks of fever, chills, abdominal pain, and jaundice. Although RPC is endemic to Southeast Asian countries, its incidence is declining in this area and increasing in the West as a result of immigration. The exact etiology of RPC is unknown, although there have been strong associations with such factors as parasitic infections, such as Clonorchis sinensis, Ascaris lumbricoides, Opisthorchis viverrini, Opisthorchis felineus, and Fasciola hepatica, low socioeconomic status, and poor nutritional status [1, 2].

As RPC is a chronic disease, patients are frequently confronted by recurrent attacks of suppurative cholangitis as well as various complications. The mass-forming complications of RPC include abscess, inflammatory pseudotumor, biloma, and cholangiocarcinoma. In general, RPC is a well-known risk factor for cholangiocarcinoma. The incidence of cholangiocarcinoma associated with RPC has been reported to be 1.5–11% [2–5]. Su et al. [4] reported that patients with cholangiocarcinoma associated with RPC had a significantly worse survival rate than those without RPC. This may be attributed to the diagnosis delay, the low diagnosis rate, previous hepatic damage caused by long-standing cholangitis, and the fact that fewer curative resections are performed for

cholangiocarcinoma. The mass-forming complications of RPC may lead to a delayed diagnosis of cholangiocarcinoma because they can be confused with cholangiocarcinoma. For early diagnosis of cholangiocarcinoma, determining how to differentiate the other mass-forming complications of RPC from cholangiocarcinoma is very important.

In recent years, MRI has become an important imaging modality for the investigation of biliary disease, as it not only provides accurate and comprehensive information but also invaluable information regarding hepatic focal lesions. For these reasons, MRI is being increasingly used to evaluate RPC as it clearly shows stones, ductal dilatation, strictures, and hepatic parenchymal complications [6–8].

Although there are some reports of CT findings for cholangiocarcinoma associated with RPC [5, 9], to our knowledge there has not been a published report of MRI findings of mass-forming complications of RPC. Therefore, in this study we have assessed the common MRI findings of mass-forming complications of RPC as well as its diagnostic performance for differentiating malignant from benign hepatic masses in patients with RPC.

Materials and methods

Patients

Our institutional review board approved this retrospective study, and patient informed consent was not required. Between November 2003 and July 2009, we performed contrast-enhanced MRI on 352 patients with histories of RPC. Among them, 65 consecutive patients had hepatic masses. Seven patients with unconfirmed masses were excluded from our study which was composed of 31 males and 27 females; mean age, 54 years; range, 45–69 years. Typical hepatic cysts and hemangiomas seen on MRI were excluded from the study. Therefore, the hepatic masses included cholangiocarcinoma (n = 15) and benign masses including abscess (n = 37), inflammatory pseudotumor (n = 3) and biloma (n = 3). All patients with cholangiocarcinoma were confirmed by hepatic lobectomy (n = 9), segmentectomy (n = 2), or biopsy (n = 4). Three patients with inflammatory pseudotumor were confirmed by biopsy (n = 1) or segmentectomy (n = 2). Thirty-seven patients with abscess and three patients with biloma were confirmed by aspiration or biopsy (n = 19), surgery (n = 6) or clinical diagnosis with imaging follow-up (n = 15). All patients with abscess had a firm clinical diagnosis, and the three patients with biloma were diagnosed by ERCP and follow-up CT or MRCP findings.

MR imaging

Contrast-enhanced MRI was performed on a 1.5-T MR system (Magnetom Sonata Maestro, Siemens Medical Solutions). Before contrast enhancement, we performed a fat suppression T1-weighted fast low-angle shot (FLASH) sequence (repetition time, 159 ms; echo time, 2.6 ms; flip angle, 120°; 7 mm slice thickness; 20 slice number), in-phase and opposed-phase gradient echo T1-weighted sequences (repetition time, 101 ms; echo time, 4.8/2.4 ms; flip angle, 70°; ETL, 1; 7 mm slice thickness; 20 slice number; matrix number, 256 × 320), a T2-weighted half-Fourier single-shot turbo spin echo (TSE) sequence (repetition time, 800; echo time, 63 ms; flip angle, 150°; 7-mm slice thickness; 20 slice number), and a T2-weighted TSE sequence (repetition time, 3595; echo time, 98 ms; flip angle, 150°; ETL, 19; 7-mm slice thickness; 24 slice number; matrix number, 384 × 312). Contrast-enhanced MR imaging was performed following administration of gadopentetate dimeglumine (Magnevist; Schering, Berlin, Germany). A dose of 0.1 mmol/kg gadopentetate dimeglumine was injected using an automated injector (Spectris MR; Medrad, Germany) at a flow rate of 3 mL/s followed by injection of 20 mL of normal saline at the same flow rate. Determination of the scan delay for image acquisition timing was achieved using the test bolus technique in which 1 mL of gadopentetate dimeglumine was injected along with a 20 mL of saline flushing. The breath-hold, T1-weighted imaging sequence for arterial phase (20–30 s), portal phase (45–60 s), and equilibrium phase (180 s) imaging was obtained using a 3D volumetric interpolated breath-hold examination (VIBE) sequence with the following parameters: repetition time, 3.4–3.8; echo time, 1.4–1.8 ms; flip angle, 12°; bandwidth, 490 Hz/Px; matrix, 256 (read) × 120 (phase) × 64–72 (partition); effective slice thickness, 2.3 mm; field of view, 32–35 cm.

Imaging interpretation

MRI was independently analyzed by two radiologists (000, 000) with 9 years of clinical experience in abdominal MR imaging. The reviewers were blinded to patient identification, clinical histories, final results, and other imaging findings. MRI scans were evaluated in random order on picture archiving and communication system (PACS) monitors.

The reviewers assessed the contrast-enhancement patterns, intratumoral appearance, peritumoral changes, any mass located in the same lobe of hepatic atrophy, a mass located in the same lobe of portal vein thrombosis or obliteration, and multiplicity of hepatic mass. The contrast-enhancement patterns included thin and lobulated enhancement at the periphery of mass, ill-defined enhancement, and multilayered target-like enhancement. Intratumoral appearance included marked low signal intensity on T1WI, cluster appearance, slightly high-signal intensity on T2WI, and any central tiny fluid-like space. The peritumoral changes included transient regional signal difference on the dynamic phase and

regional high-signal intensity on T2WI. They also measured the long diameter of each mass. The reviewers then rated the likelihood of a malignant mass in each patient by means of statistically common MR findings for malignant and benign masses using a five-point scale as follows: 1, definitely benign; 2, probably benign; 3, indeterminate; 4, probably malignant; and 5, definitely malignant. When the readers' interpretations differed, a third opinion (000) was obtained.

Statistical analysis

The Chi-square test was used to compare each MRI findings. A P value less than 0.05 were considered to indicate a significant difference. The diagnostic performance of MR imaging for differentiating malignant from benign masses was expressed using the area under the receiver operating characteristic (ROC) curve (A_z). Interobserver agreement was evaluated using the κ statistic. A κ value less than 0.20 was considered poor; 0.21–0.4, fair; 0.41–0.60, moderate; 0.61–0.80, good; and 0.81–1.00 excellent. Statistical analysis was conducted using SPSS version 11.5 software (SPSS, Chicago, IL, USA).

Results

The long diameter of a malignant mass (5.02 ± 2.02 cm) was larger than a benign mass (3.38 ± 1.84 cm, P = 0.005). Table 1 summarizes the MRI findings of malignant and benign hepatic masses. The statistically common findings for cholangiocarcinoma compared with those of a benign mass were as follows: thin and lobulated enhancement at the periphery (n = 8, 53%, P < 0.05); ill-defined enhancement (n = 7, 47%, P < 0.05); slightly high-signal intensity on T2WI (n = 13, 87%, P < 0.05); mass located in the same lobe as the hepatic atrophy (n = 11, 73%, P < 0.05); and mass located in the same lobe as the portal vein thrombosis or obliteration (n = 15, 100%, P < 0.05). The most common MRI finding for cholangiocarcinoma was that of a mass located in the same lobe as the portal vein thrombosis or obliteration (Fig. 1); this was seen in 15 patients (100%) with cholangiocarcinoma and in 15 patients (35%) with a benign mass. A mass located in the same lobe as the hepatic atrophy was seen in 11 patients (73%) with cholangiocarcinoma and in four patients (9%) with benign masses. Slightly high-signal intensity on T2WI was seen in 13 patients (87%) with cholangiocarcinoma and in 17 patients (40%) with benign masses (Fig. 2).

The statistically common findings for a benign mass compared with cholangiocarcinoma were as follows: multilayered target-like enhancement (n = 36, 84%, P < 0.05); cluster appearance (n = 15, 35%, P < 0.05); central fluid-like space (n = 29, 67%, P < 0.05); peritumoral regional high-signal intensity on T2WI (n = 32, 74%, P < 0.05); and multiplicity (n = 21, 49%, P < 0.05). The most common MRI finding for a benign mass was multilayered target-like enhancement (Fig. 3); this was seen in 36 patients (84%) with a benign mass and was not seen in those with cholangiocarcinoma. A cluster appearance was also seen only in benign masses. Peritumoral regional high-signal intensity on T2WI was seen in 32 patients (74%) with benign masses and in five patients (33%) with cholangiocarcinoma. Twenty-six patients with peritumoral regional high-signal intensity on T2WI combined transient signal intensity differences at the same site. Thirteen of 32 (41%) patients with peritumoral regional high-signal intensity on T2WI and 16 of 34 (47%) patients with transient regional-signal difference on the dynamic phase were accompanied by thrombosis of the regional portal vein or hepatic vein (Fig. 4). Three cases of inflammatory pseudotumor showed thin and lobulated enhancement at the periphery of hepatic mass (n = 2) (Fig. 5), ill-defined enhancement (n = 1), and low signal intensity on T1WI (n = 2). The κ values for the two reviewers, which were calculated for each MRI finding, ranged from 0.81 to 1.00. Interobserver agreement was excellent with regard to each MRI finding.

Table 1. MR imaging findings of malignant and benign hepatic masses in patients with recurrent pyogenic cholangitis

MR findings	Malignant mass (n = 15)	Benign mass (n = 43)	P
Enhancement patterns			
Thin peripheral enhancement	8 (53%)	4 (9%)	P < 0.05
Ill-defined enhancement	7 (47%)	3 (7%)	P < 0.05
Multilayered target-like enhancement	0	36 (84%)	P < 0.05
Intratumoral appearance			
Cluster appearance	0	15 (35%)	P < 0.05
Central fluid-like space	1 (6%)	29 (67%)	P < 0.05
Marked low SI on T1WI	10 (67%)	17 (40%)	P = 0.07
Slightly high SI on T2WI	13 (87%)	17 (40%)	P < 0.05
Peritumoral changes			
Transient SI difference	13 (87%)	34 (79%)	P = 0.51
Peritumoral regional high SI on T2WI	5 (33%)	32 (74%)	P < 0.05
Mass located in same lobe as the hepatic atrophy	11 (73%)	4 (9%)	P < 0.05
Mass located in same lobe as the portal vein thrombosis	15 (100%)	15 (35%)	P < 0.05
Multiplicity	2 (13%)	21 (49%)	P < 0.05

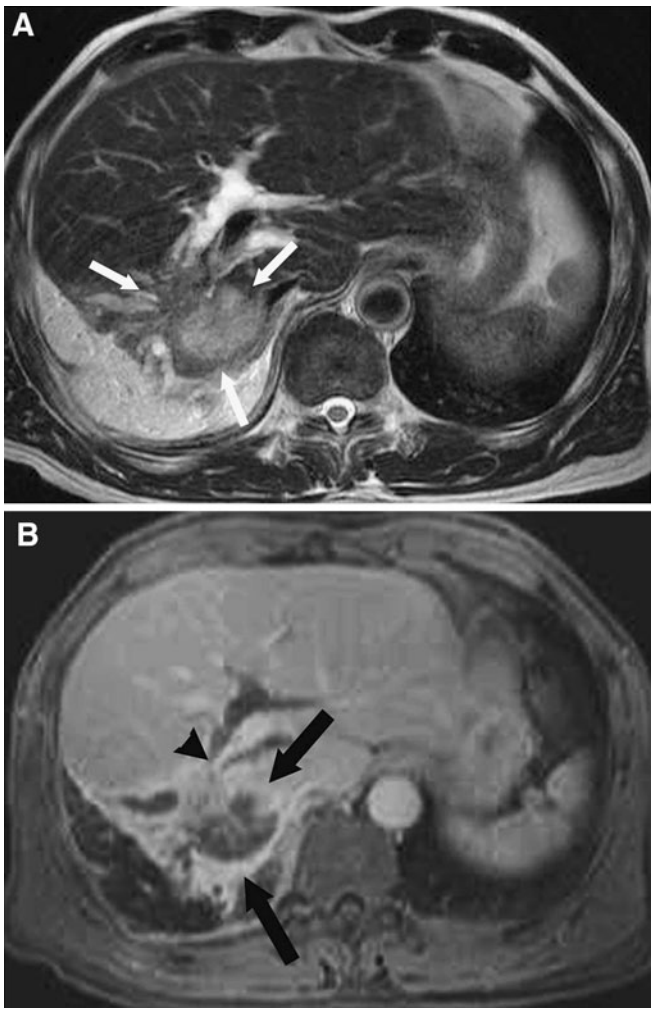

Fig. 1. Cholangiocarcinoma associated with RPC in a 65-year-old-man who complained of abdominal pain and fever. **A** T2-weighted TSE MR image demonstrates slightly high-signal intensity mass (*arrows*). **B** Contrast-enhanced MR image during the equilibrium phase shows a thin enhancement at the periphery of the mass (*arrows*). The mass located in the same lobe as the hepatic atrophy and the portal vein obliteration (*arrowhead*). The diagnosis of cholangiocarcinoma was made by percutaneous liver biopsy.

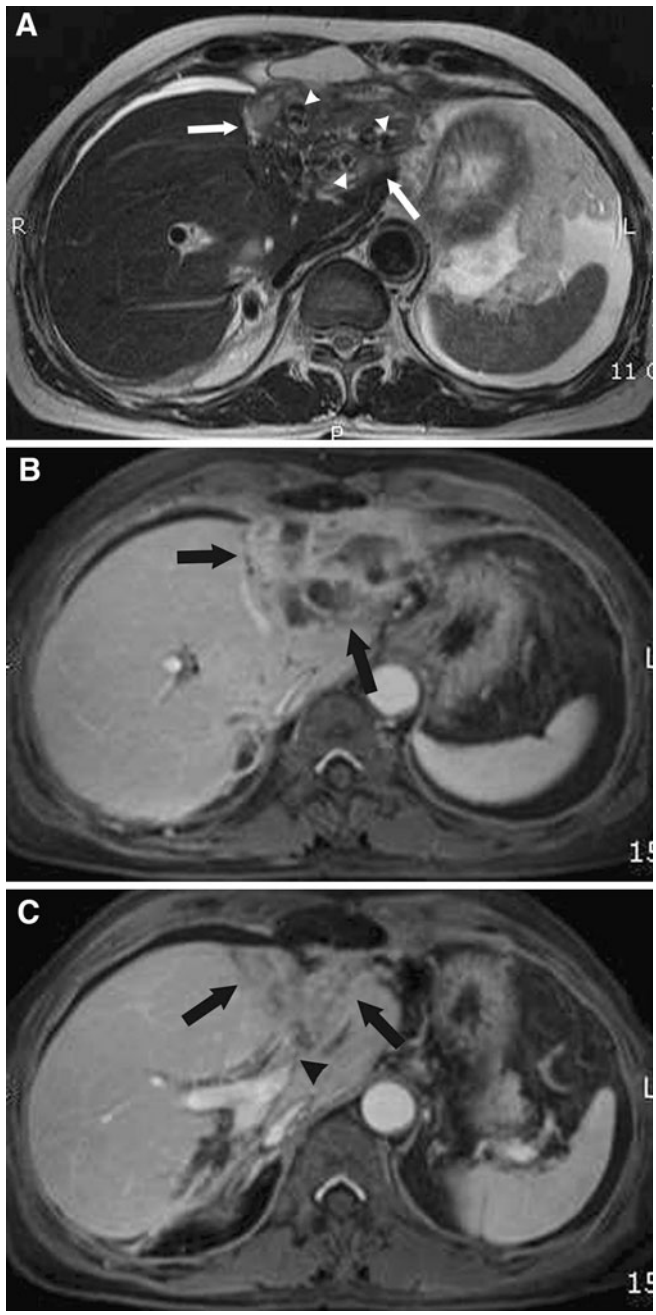

Fig. 2. Cholangiocarcinoma associated with RPC in a 67-year-old man who complained of abdominal pain, fever, and leukocytosis. He had a history of recurrent attacks of the cholangitis and clonorchis sinensis infestation. **A** T2-weighted TSE MR image demonstrates slightly high-signal intensity mass (*arrows*) in the lateral segment of the left lobe. There are hepatolithiasis within the intrahepatic duct (*arrowheads*). **B**, **C** Contrast-enhanced MR images during the portal phase show an ill-defined enhancement of the mass (*arrows*). The mass located in the same lobe as the portal vein obliteration (*arrowhead*). The diagnosis of cholangiocarcinoma was made by surgical resection.

The area under the ROC curve (Az) for MR diagnostic performance to differentiate malignant from benign masses by means of statistically common MR findings was 0.989, and using the cut-off point as 3, the sensitivity was 95.3% and the specificity was 95.3% (Fig. 6). Interobserver agreement was good ($\kappa = 0.74$).

Discussion

Cholangiocarcinoma has become an important, late complication of RPC. Cholangiocarcinoma associated

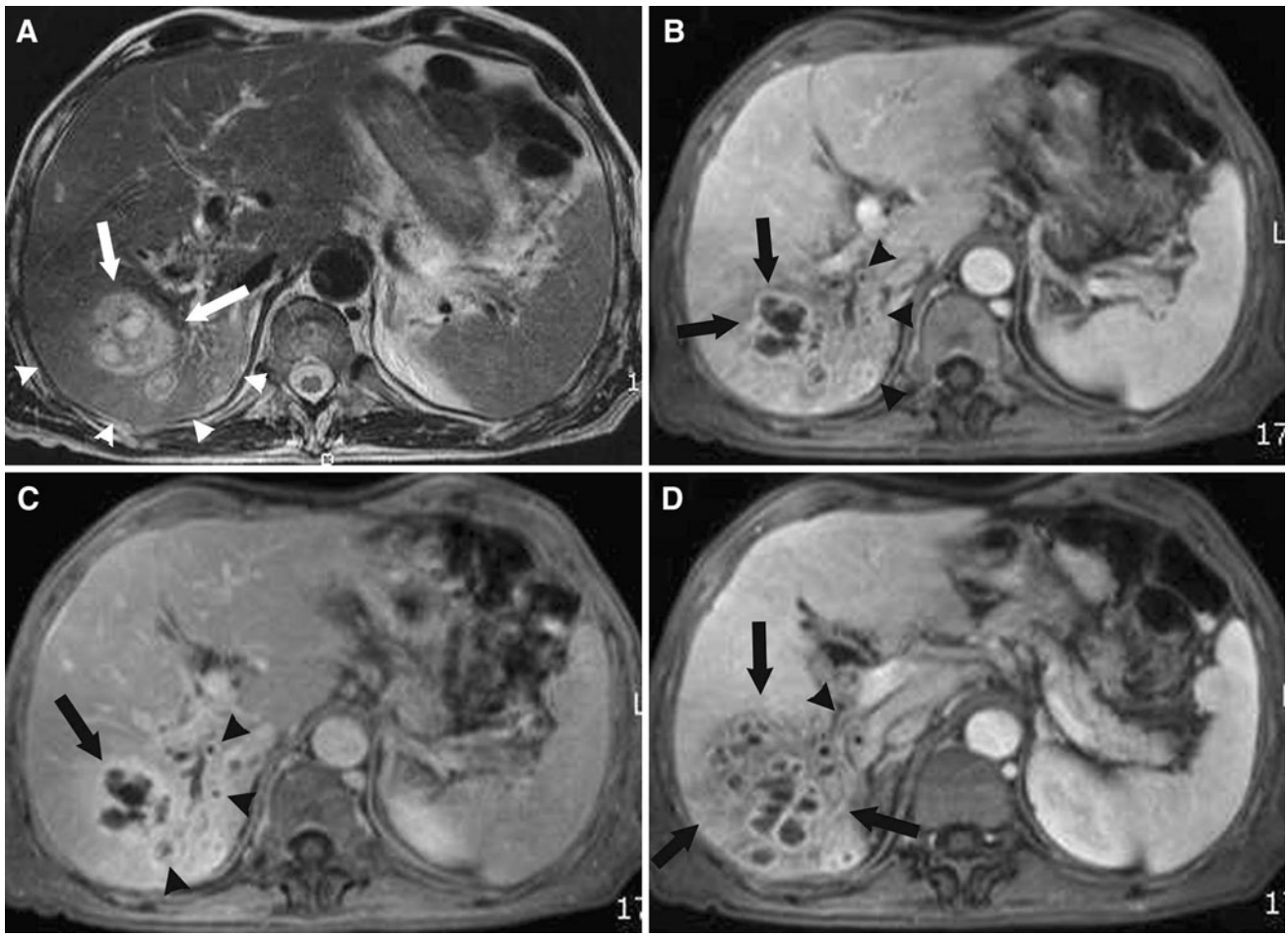

Fig. 3. Hepatic abscess associated with RPC in a 59-year-old woman who complained of abdominal pain, fever, and leukocytosis. She had a history of recurrent attacks of cholangitis. **A** T2-weighted TSE MR image demonstrates a mass in the right lobe with central fluid-like space (*arrows*). This mass shows peritumoral regional high-signal intensity (*arrowheads*). **B**, **C** Contrast-enhanced MR images during the portal phase and the equilibrium phase show multilayered target-like enhancement of the mass (*arrows*). There are multiple small lesions in the right lobe (arrowheads). MR image (**D**) obtained 16 mm below (**B**) shows clustered multiple small abscesses (*arrows*) in the right lobe. There is thrombosis in the right portal vein (*arrowhead*). This mass was confirmed as an abscess by aspiration.

with RPC has a poor prognosis due to the often delayed diagnosis, a low diagnosis rate, and fewer curative resections. It is also difficult to make an accurate diagnosis before treatment. The imaging features of RPC include bile duct dilatation, bile duct stricture, biliary calculi, hepatic atrophy, portal vein obliteration, and mass-forming complications such as hepatic abscess, biloma, and inflammatory pseudotumor which may lead to the delayed diagnosis of cholangiocarcinoma associated with RPC as they may obscure an underlying cholangiocarcinoma [3, 4, 10, 11]. Our study results showed that statistically common findings for cholangiocarcinoma included thin and lobulated enhancement at the periphery of hepatic mass, ill-defined enhancement, slightly high-signal intensity on T2WI, and a mass located in the same lobe as the hepatic atrophy and portal vein thrombosis or obliteration. Statistically common findings for a benign mass included multilayered target-like enhancement, a cluster appearance, a central fluid-like space, peritumoral regional high-signal intensity on T2WI, and multiplicity. Using these specific MRI findings, the area under the ROC curve was 0.989, the sensitivity was 95.3%, and the specificity was 95.3% with good interobserver agreement.

In our study patients, cholangiocarcinoma tended to occur in the same segment as the portal vein thrombosis or atrophied segments. Cholangiocarcinoma located in the same lobe as the portal vein thrombosis or obliteration was seen in 15 patients (100%), whereas a benign mass located in the same lobe as the portal vein thrombosis was seen in 15 patients (35%, $P < 0.05$). Cholangiocarcinoma located in the same lobe as the hepatic atrophy was seen in 11 patients (73%) with cholangiocarcinoma and in four patients (9%, $P < 0.05$) with

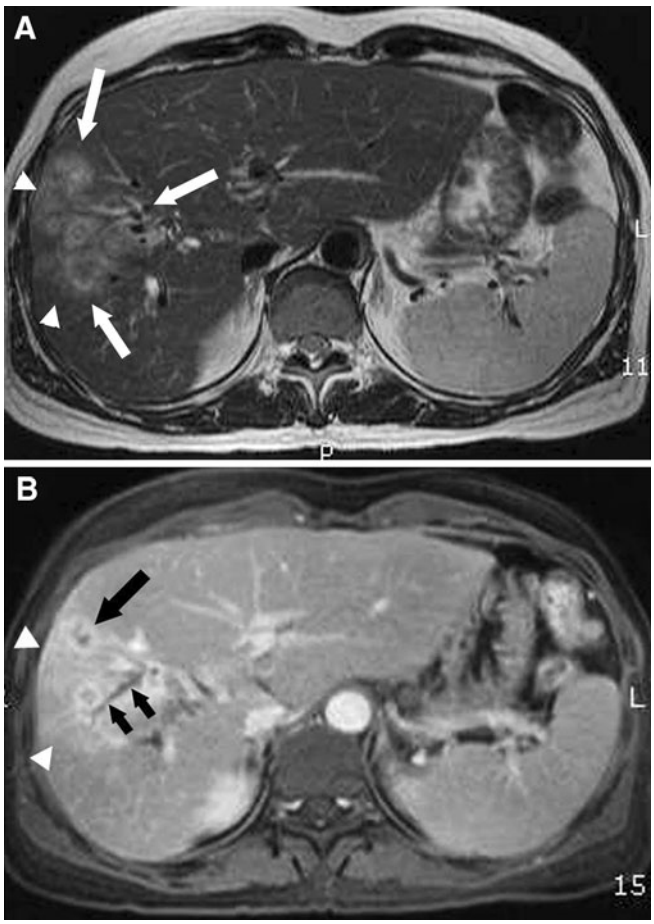

Fig. 4. Hepatic abscess associated with RPC in a 53-year-old man who complained of abdominal fever and leukocytosis. He had a history of recurrent attacks of cholangitis. **A** T2-weighted TSE MR image shows multiple small lesions in the anterior segment of the right lobe (*arrows*) with peritumoral regional high-signal intensity (*arrowheads*). **B** Contrast-enhanced MR images during the portal phase demonstrate multilayered target-like enhancement of the mass (*large arrow*). There are transient signal intensity differences at the same site as peritumoral regional high-signal intensity on T2WI (*arrowheads*). Note thrombosis at the braches of middle hepatic vein (*small arrows*). This mass was confirmed as an abscess by aspiration.

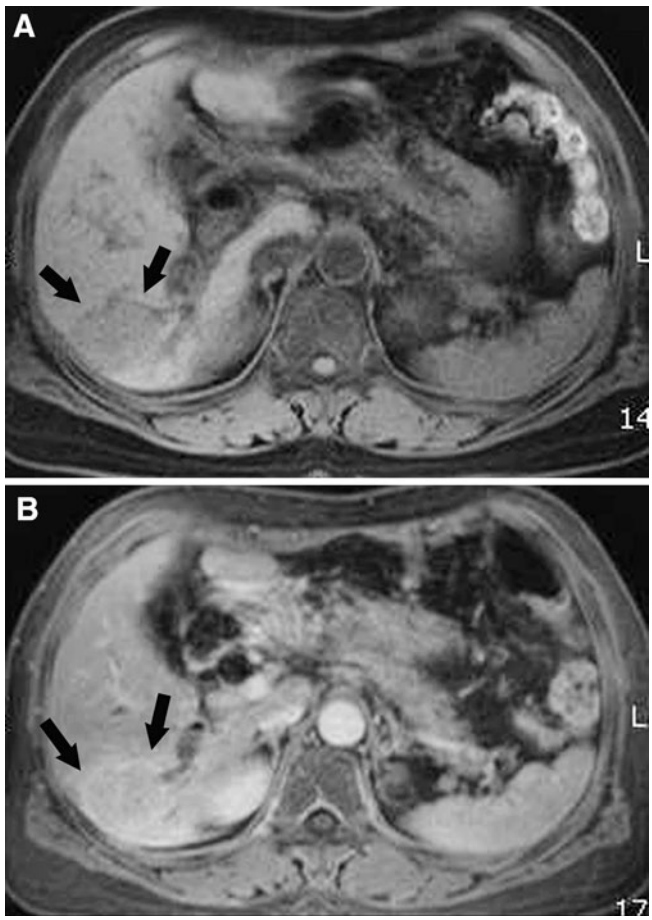

Fig. 5. Hepatic inflammatory pseudotumor associated with RPC in a 51-year-old woman who complained of abdominal pain and fever. She had a history of recurrent attacks of cholangitis. **A** T1-weighted fat suppression FLASH MR image demonstrates low signal intensity mass (*arrows*) in the posterior segment of the right lobe (*arrows*). **B** Contrast-enhanced MR image during the portal phase shows a thin and lobulated enhancement at the periphery of the mass (*arrows*). The diagnosis of cholangiocarcinoma was made by surgical resection.

benign masses. Kim et al. [5] that reported cholangiocarcinoma associated with RPC was found to predominantly localize in segments with atrophy and with narrowing or obliteration of the portal vein. In Kim's study, the coincident rate of peripheral cholangiocarcinoma in hepatic atrophy was 88% and that in portal vein narrowing or obliteration was 83%; this is consistent with our results. The primary hypothesis regarding cholangiocarcinoma associated with RPC is that parasitic infections lead to the initial epithelial damage which may then lead to inflammatory and fibrotic changes in bile duct walls that result in stricture, bile stasis, and intrahepatic stone formation. The mechanical irritation caused by biliary stones can lead to the development of mucosal adenomatous hyperplasia and chronic proliferative cholangitis which can undergo progressive change to atypical epithelial hyperplasia and ultimately to cholangiocarcinoma. During episodes of recurrent cholangitis, thrombophlebitis of portal vein branches is common and can result from intimal fibrosis secondary to inflammatory changes in the adjacent periportal spaces. As long-lasting intrahepatic duct obstruction or portal vein thrombosis may result in lobar or segmental atrophy, the segment of portal vein thrombosis or atrophied segments suggest areas of long-lasting recurrent cholangitis which are vulnerable to cholangiocarcinoma [4, 12, 13].

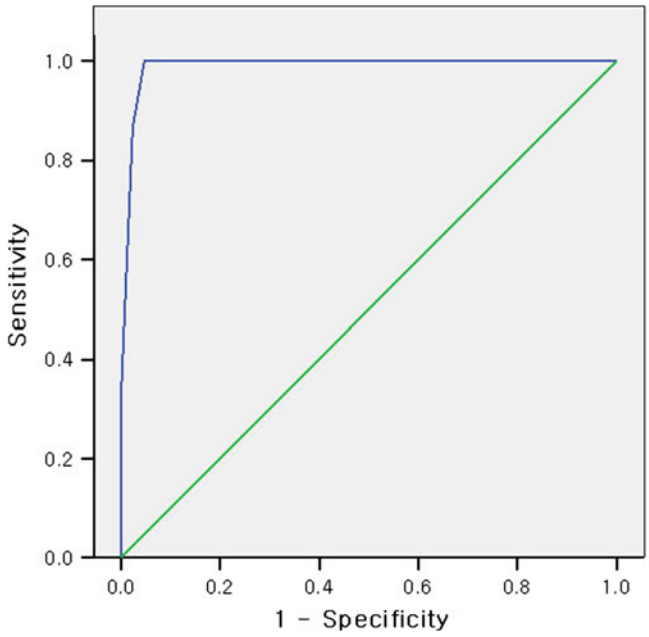

Fig. 6. Receiver operating characteristics curve for MR diagnostic performance to differentiate malignant from benign masses by means of statistically common MR findings. The area under the curve is 0.989.

In our study, the most common benign hepatic mass in RPC was abscess (n = 37, 86%). According to a previous report, hepatic abscesses have been detected in up to 20% of patients with RPC [14]. Multilayered target-like enhancement is the most common MRI finding in a benign mass and was seen in 36 of our study patients (84%) with benign masses but was not seen in those with cholangiocarcinoma. A cluster appearance and central fluid-like space were also commonly seen in 15 (35%) and 29 patients (67%) with benign masses, whereas only one patient with cholangiocarcinoma showed a central fluid-like space on MRI. According to previous reports [15–17], multilayered target-like enhancement, the so-called double-target sign, was found in 30% of the abscesses reported by Mathieu et al. [15] and in 42% of the abscesses reported by Gabata et al [16] who mentioned that the pathology of the wall of abscess cavity indicates a three-layer structure, fresh granulation tissue, old fibrous-granulation tissue, and an outer inflammatory edema area. Therefore, multilayered target-like enhancement seen on MRI might represent these pathologic structures, whereas small abscesses have a tendency to cluster or aggregate, the so-called cluster sign, and coalesce into a single larger abscess cavity [17].

Peritumoral regional high signal intensity on T2WI was seen in 32 patients (74%) with benign masses and in five patients (33%, $P < 0.05$) with cholangiocarcinoma. Transient regional-signal difference on the dynamic phase was seen in 34 patients (79%) with benign masses and in 13 patients (87%, $P = 0.51$) with cholangiocarcinoma. In benign hepatic masses, 26 patients with peritumoral regional high-signal intensity on T2WI combined a transient regional signal difference at the same site. Mathieu et al. [15] also reported that the hepatic parenchyma surrounding an abscess showed transient segmental or wedge-shaped enhancement on the arterial dominant phase of dynamic CT in 12 (30%) of 40 patients. They hypothesized that this transient enhancement was a result of localized hepatic venous obstruction caused by acute inflammation of the hepatic parenchyma surrounding the abscess. Hanazaki et al. [18] proposed that hepatic abscess may lead to infectious damage of the portal vein which might result in thrombosis. This hypothesis was reinforced by Gabata et al. [16] who reported marked periportal inflammation and stenosis of the portal venules surrounding hepatic abscesses, which may result in the reduction of portal flow and a compensatory increase in arterial inflow. Under these circumstances, dynamic-enhanced imaging can detect transient regional enhancement around the abscess [15, 16]. In our study, 13 of 32 (41%) patients with peritumoral regional high-signal intensity on T2WI and 16 of 34 (47%) patients with transient regional-signal difference were accompanied by thrombosis of the regional portal vein or hepatic vein.

Multiplicity was observed in 21 patients (49 %) with benign masses and in two patients (13 %) with cholangiocarcinoma. Alvarez et al. [19] reported that among 133 cases with liver abscesses, 27.1% had multiple lesions. Zibari et al. [20] reported that among 20 cases with liver abscesses, 30% had multiple lesions. Our three cases of inflammatory pseudotumor show thin and lobulated enhancement at the periphery of hepatic mass (n = 2), ill-defined enhancement (n = 1), and low SI on T1WI (n = 2). These findings are similar to those for cholangiocarcinoma. Using imaging findings alone, it may be difficult to differentiate inflammatory pseudotumor from cholangiocarcinoma. In our study, three patients with inflammatory pseudotumor were confirmed by biopsy (n = 1) and surgery (n = 2).

Our study does have some limitations. First, the number of cholangiocarcinomas is relatively small compared to benign masses. As cholangiocarcinoma associated with RPC is uncommon, it is an inevitable limitation. Secondly, while surgical correlation was not available in all of our study patients, many cases of benign masses required no further invasive procedures or surgery; however, in these cases we had a firm clinical diagnosis and imaging follow-up.

Despite these limitations, our study suggests several unique MR findings regarding mass-forming complications associated with RPC. Our study results showed that cholangiocarcinoma tended to occur in the same segment of the portal vein thrombosis or in atrophied segments and those statistically common findings of cholangiocarcinoma included thin and lobulated enhancement at the periphery, ill-defined enhancement, and slightly high-

signal intensity on T2WI. Statistically common findings for benign masses included multilayered target-like enhancement, a cluster appearance, central fluid-like space, peritumoral regional high-signal intensity on T2WI, and multiplicity. These specific MRI findings should be recognized as they improve the early diagnosis rate and proper treatment of patients with RPC. Correlation with clinical and laboratory findings is warranted as benign inflammatory processes can mimic malignancy.

In conclusion, because of the statistically common MRI findings for cholangiocarcinoma and benign hepatic masses, MRI is very useful for the differential diagnosis of malignant vs. benign hepatic masses in patients with RPC.

Acknowledgment. We would like to thank Bonnie Hami, MA (USA) for her editorial assistance in the preparation of the manuscript.

References

1. Lim JH (1991) Oriental cholangiohepatitis: pathologic, clinical, and radiologic features. AJR Am J Roentgenol 157:1–8
2. Carmona RH, Crass RA, Lim RC Jr, Trunkey DD (1984) Oriental cholangitis. Am J Surg 148:117–124
3. Chen MF, Jan YY, Wang CS, et al. (1993) A reappraisal of cholangiocarcinoma in patients with hepatolithiasis. Cancer 71:2461–2465
4. Su CH, Shyr YM, Lui WY, P'Eng FK (1997) Hepatolithiasis associated with cholangiocarcinoma. Br J Surg 84:969–973
5. Kim JH, Kim TK, Eun HW, et al. (2006) CT findings of cholangiocarcinoma associated with recurrent pyogenic cholangitis. AJR Am J Roentgenol 187(6):1571–1577
6. Kim MJ, Cha SW, Mitchell DG, et al. (1999) MR imaging findings in recurrent pyogenic cholangitis. AJR Am J Roentgenol 173: 1545–1549
7. Park MS, Yu JS, Kim KW, et al. (2001) Recurrent pyogenic cholangitis: comparison between MR cholangiography and direct cholangiography. Radiology 220:677–682
8. Jain M, Agarwal A (2008) MRCP findings in recurrent pyogenic cholangitis. Eur J Radiol 66(1):79–83
9. Radin DR, Ray MJ, Ralls PW, Boswell WD Jr, Halls JM (1987) Hepatolithiasis complicated by cholangiocarcinoma. J Comput Tomogr 11:315–317
10. Kubo S, Kinoshita H, Hirohashi K, Hamba H (1995) Hepatolithiasis associated with cholangiocarcinoma. World J Surg 19:637–641
11. Sheen-Chen SM, Chou FF, Eng HL (1991) Intrahepatic cholangiocarcinoma in hepatolithiasis: a frequently overlooked disease. J Sur Oncol 37:131–135
12. Chijiiwa K, Ichimiya H, Kuroki S, Koga A, Nakayama F (1993) Late development of cholangiocarcinoma after the treatment of hepatolithiasis. Surg Gynecol Obstet 177:279–282
13. Ohta T, Nagakawa T, Ueda N, et al. (1991) Mucosal dysplasia of the liver and the intraductal variant of peripheral cholangiocarcinoma in hepatolithiasis. Cancer 68:2217–2223
14. Tsui WM, Chan YK, Wong CT, et al. (2011) Hepatolithiasis and the syndrome of recurrent pyogenic cholangitis: clinical, radiologic, and pathologic features. Semin Liver Dis 31:33–48
15. Mathieu D, Vasile N, Fagniez PL, et al. (1985) Dynamic CT features of hepatic abscesses. Radiology 154:749–752
16. Gabata T, Kadoya M, Matsui O, et al. (2001) Dynamic CT of hepatic abscesses: significance of transient segmental enhancement. AJR Am J Roentgenol 176:675–679
17. Jeffrey RB Jr, Tolentino CS, Chang FC, Federle MP (1988) CT of small pyogenic hepatic abscesses: the cluster sign. AJR Am J Roentgenol 151:487–489
18. Hanazaki K, Kajikawa S, Nagai N, et al. (2001) Portal vein thrombosis associated with hilar bile duct carcinoma and liver abscess. Hepatogastroenterology 48:79–80
19. Alvarez JA, Gonzalez JJ, Baldonedo RF, et al. (2001) Single and multiple pyogenic liver abscesses: etiology, clinical course, and outcome. Dig Surg 18:283–288
20. Zibari GB, Maguire S, Aultman DF, McMillan RW, McDonald JC (2000) Pyogenic liver abscess. Surg Infect (Larchmt) 1:15–21